Punching Shear Strength of Self Compacted Ferrocement Slabs

Abdulkhaliq Abdulyimah Jaafer
Lecturer
College of Engineering- Misan University
E mail: aljabery@uomisan.edu.iq
aljabery_1981@yahoo.com

Sa'ad Fahad Resan
Lecturer
College of Engineering- Misan University
E mail: sadresan@uomisan.edu.iq

ABSTRACT

This study aims to investigate the behavior and strength of self-compacted ferrocement slabs under punching shear load. Experimental results of thirteen square ferrocement slabs of 500×500 mm simply supported on all edges are presented. The main parameters investigated include the volume fraction of reinforcement, slab thickness and size of load-bearing plate. The load deflection and cracking characteristics of the tested slabs are studied and compared. The test results showed that the volume fraction of wire mesh has significant effect on both ultimate load and displacement. The increase of slab thickness leads to decrease in deflection values and increase in stiffness of slabs. Both ductility and stiffness increase as the loaded area size is increased.

Key words: self compacting mortar, ferrocement, punching shear, slabs, volume fraction

مقاومة القص الثاقب للبلاطات الفيروسمنتيه ذاتية الرص

د. سعد فهد رسن
مدرس
كلية الهندسة ـ جامعة ميسان

د.عبدالخالق عبداليمه جعفر
مدرس
كلية الهندسة ـ جامعة ميسان

الخلاصة

تهدف هذه الدراسة الى تحري سلوك ومقاومة البلاطات الفيروسمنتيه ذاتية الرص تحت تاثير حمل القص الثاقب. استعرضت الدراسة نتائج عمليه لثلاثة عشر بلاطة فيروسمنتيه مربعة الشكل بابعاد (500×500 ملم) وبسيطة الاسناد من جميع الجهات. تضمنت دراسة المتغيرات الرئيسية وهي النسبة الحجميه للتسليح, سمك البلاطة وحجم لوحة التحميل. وكذلك تم دراسة خصائص منحنى الحمل-التشوه وخصائص التشقق للبلاطات المفحوصة. بينت الدراسة ان النسبة الحجميه للتسليح لها تاثير كبير على كل من الحمل الاقصى والتشوه الاقصى. كما ان الزيادة في السمك تؤدي الى زيادة في جساءة البلاطة ونقصان في الهطول. و ان كلا من المطيلية والجساءة يزدادان بزيادة ابعاد لوحة التحميل.

الكلمات الرئيسيه: ملاط ذاتي الرص, فيروسمنت, القص الثاقب , بلاطات, الكسور الحجميه.

1. INTRODUCTION

Ferrocement is a type of thin wall reinforced concrete commonly constructed of hydraulic cement mortar reinforced with closely spaced layers of continuous and relatively small size wire mesh. The mesh may be made of metallic or other suitable materials **ACI Committee 549, 1999**. Ferrocement has a very high tensile strength-to-weight ratio and superior cracking behavior in comparison to conventional reinforced concrete. This means that thin ferrocement structures can be made relatively light and watertight. Hence, ferrocement is an attractive material for the construction of prefabricated housing units, boats, barges, and other portable structures **ACI, Committee 549, 1999**.

Also, ferrocement can be utilised in a number of practical application such as repair, rehabilitation and strengthening of different concrete structural members **Lub and Van, 1989, Fahmy and Shaheen, 1994, Romualdi et al., 1998, Fahmy et al., 1999, Razali et al., 2005, Dongyen et al., 2006, Jeyasehar and Vidivelli, 2006,** and **Shannag 2009**.

Recent and interesting applications are related to the adoption of self compacting mortar in the field of retrofitting and strengthening of reinforced concrete structures **Kazim, 2012**. It is preferred due to the easiness of application and mechanical advantages. The applied mortar to the structural members is usually hard to consolidate and vibration is not possible in most cases **Rathish and Srikanth, 2008**. In addition to these, the self-compactability of mortars may provide considerable advantages such as reducing the construction time and labor cost, enhancing the filling capacity of highly congested structural members **Kazim, 2012**.

Therefore, an experimental study is performed on self compacted cementitious slabs and reinforced with welded steel wire mesh to investigate its strength and behavior under patch loading. There are limited investigations that have been carried out to study the behavior of ferrocement members under punching shear. These include **Paramasivam and Tan, 1993, Al-Kubaisy and Jumaat, 1999, Mansur et al., 2000** and **2001, Ibrahim, 2011**.

Due to the limited studies, this paper is aimed to investigate the behavior and strength of self-compacted ferrocement slabs under punching shear load. The main parameters considered in this study include the volume fraction of reinforcement, overall thickness, and the size of the load bearing plate. Thirteen ferrocement slabs are tested. The results of these tests are presented and the influences of various parameters on the punching shear strength are discussed. The load-deflection of these slabs is also discussed in this paper.

2. EXPERIMENTAL PROGRAMS

2.1. Specimen Details and Test Parameters

A total of thirteen ferrocement slabs of identical length and width but different depths have been tested in the Construction Materials Laboratory of the College of Engineering at University of Misan. The casted slabs were 500 mm long × 500 mm wide with two different depths of 30 and 45 mm.   The specimens comprised of two control ferrocement slabs cast with ordinary mortar and the other eleven made with self compacting mortar. Specimen details and main study parameters are summarized in **Table 1**. The slab specimens were simply supported along the four edges with corners free to lift and free to rotate about the support axes as shown in test setup in **Fig. 1**. The support-to-support span (l) for all the slabs was 400mm in each direction. The load has been applied by means of a hydraulic jack as shown in **Fig. 1**. A square rigid steel plate with side (w) of (40 and 80 mm) was placed between the jack and slab to apply the load in the center of the slab. A mechanical dial gauge was placed at the center of the slab to measure the vertical displacement while a calibrated load cell was used to record the load as shown in **Fig. 1**.

2.2. Materials and Mixing Proportions

Welded square wire mesh with a wire diameter of 1.0 mm and 12.5 mm spacing was provided as an internal reinforcement for ferrocement slabs. The mesh was tested according to the design guide on construction and repair of ferrocement reported by the **ACI committee 549, 1999**. The yield strength of the wire mesh was determined to be 405 MPa. The average ultimate strength of the wire mesh and modulus of elasticity was found to be 600 MPa and 95 GPa, respectively as shown in **Table 2**. Mortar matrix consisted of ordinary Portland cement locally available and natural sand with specific gravity of 2.60. In the mix, 10% by weight of cement was replaced by silka fume. The water and sand to binder ratios by weight were chosen to be 0.3 and 1.0 respectively. Supperplastcizer type **Sika Viscocrete ,2010,** was used as high range water reducer. The dose of superplasticizer used to obtain self compacted mortar was 3% by total binder weight. Potable water was used in the experimental work for both mixing and curing.

2.3. Mortar Mixing and Fresh Properties Tests

The batch of mortar was produced using rotating drum type of half bag capacity. The Portland cement and silica fume were initially dry mixed at low mixing speeds prior to the addition of other constituent materials. Further mixing sequences and durations were performed in accordance to standard procedures prescribed in **ASTM Standard C305**, **1999.**

After the mixing was completed, tests were conducted on fresh self compacting mortar to determine mini slump flow diameter and mini V-funnel flow time as shown in **Fig. 2.** The mini slump flow diameter and mini V-funnel flow time of self compacted mortar were presented in **Table 3**. Segregation and bleeding were visually checked during the slump flow test and was not observed.

2.4. Fabrication of Test Specimens

 The wooden moulds dimensions were (500x500x30 or 45mm). The desired mesh layers were tied by fine steel wires and then placed inside the moulds. Fresh mortar mix was then poured into the wooden mould as shown in **Fig. 3**. Along with the slabs, a total of six (50x50x50 mm) mortar cubes and three (40x40x160 mm) mortar prisms were moulded. The mortar specimens were used for compressive and flexure strength tests. The matrix characterised by an average compressive and flexural strength of 70 and 7.7 MPa, respectively. Moulded specimens were cured in mould for 24 hour and then removed from their moulds, and immersed in the curing tank for 28 days.

 Before the testing day, the slab was cleaned and painted with white paint on both surfaces, to achieve clear visibility of cracks during testing. The slab was carefully placed on the simple supports. The point load was applied at the centre of the top surface of the slab and the dial gauge was positioned under the centre of the bottom surface of the slab, so that a precise set-up of the testing equipment was achieved.

3. TEST RESULTS AND DISCUSSION

3.1. General Behavior

The general behavior of self compacting ferrocement slabs and normal ferrocement slabs are all nearly identical as shown in **Figs. 4** and **5**. When the load is applied to the slab specimen, the first visible crack (bending cracks) was observed at the tension face of the tested slab and the relationship between load and displacement is linear till flexural cracks occur. In all slabs, cracking on the tensile face began near the center and radiated towards the edges (semi-random phenomena). As the load is increased the cracking propagated to the opposite face. At higher

loads, the already formed cracks got widened while new cracks started to form. The new formed cracks are roughly semi-circular or elliptical in shape and occurred in the tension surface of the slab. Failure of the slab occurred when the cone of failure radial outward from the point of load application pushed up through the slab body (brittle failure with limited warning). At failure, the slab was no longer capable of taking additional load.

3.2. Cracking and Failure Patterns

 Fig. 6 presents general patterns cracking and failure on the top and bottom faces of the self compacted and normal specimens after failure. No cracks are observed in the compression face of any slab, except those which are observed around the loaded area at failure, which are almost the same as that of the loading plate dimensions. The cracks on the bottom face of specimens are radial, propagating from the centre of slab. These patterns are occurred at the center of slabs and propagated across the slab to the sides in the redial direction. Different cracking patterns may be noticed in **Figs. 7** to **9** such as spacing, extent of cracks and perimeter of failure cone. These variations depending on the volume fraction of wire mesh, the thickness of specimens and size of loading plate. It can be noticed that combined flexural-punching failure mode is found in slabs with small amount of reinforcement ratio and pure punching shear failure is found in specimens that have moderate and high volume fraction. The crack patterns at failure became more closely spaced with increasing the reinforcement content.

3.3. Load-Deflection Response

The load-displacement relationships for self compacted ferrocement slabs and corresponding control (normal ferrocement) slabs are presented in **Figs. 4** and **5**. It can be noticed from these figures, that relationships are approximately identical at all loading stages. **Fig. 10** shows load-displacement relationship of the control slab (0-45-S) that it tested under patch load to determine the ultimate load carrying capacity of plain mortar specimen. When adding wire mesh of volume fraction (0.77, 1.154, 2.31 and 3.464 %) for slabs (2-45-S, 3-45-S, 4-45-S, 6-45-S and 9-45-S) respectively, the ultimate load increases (155, 188,366, 533 and 658%) respectively, as shown in **Fig. 11** and **Table 4**. It may be seen from **Fig. 11** that the specimen (9-45-S) with the high volume fraction has highest ultimate shear load and stiffness but less ductility when it is compared with the specimen with lower reinforcement ratio (2-45-S). This proves that the volume fraction of wire mesh has significant effect on both ultimate load and displacement at ultimate load.

      Figs. 12 and **13** illustrate the load-deflection relationships of slabs with different size of loading plate. As it is clear from these figures, the increase of the loading plate size leads to increase of ultimate loads. The effect of the loading plate size on the ultimate shear load with various volume fractions is shown in **Fig. 14**. As shown in this figure, the increase of size causes an increasing in the ultimate strength of slabs. For slabs having volume fraction (1.154 and 2.31 %), the ultimate capacity is increased by (24 and 29%) respectively, when loading plate changed from 40 to 80 mm, respectively. The behavior of slabs of different thicknesses and reinforced with same volume fraction is denoted in **Figs. 15** to **17**.
The increase of slab thickness leads to decrease in deflection values at each stage of loading. **Fig. 18** shows the effect of the volume fraction on ultimate load of self compacted ferrocement slab. It is obvious from this figure that the ultimate capacity of the slabs increases with the increase of the thickness of slab at the same amount of reinforcement ratio.

51

4. PREDICTION OF PUNCHING SHEAR STRENGTH

Many codes and researchers have presented different formulas for predicting the punching shear strength of concrete slabs but no any code provision for punching shear in ferrocement. For concrete slabs, most codes present formulas, where the design punching load is a product of design nominal shear strength by the critical punching shear perimeter and the effective depth of the slab. The critical perimeter of punching shear depends on the shape of critical perimeter and its distance from loaded face. The characteristics of critical punching shear perimeter that considered in different codes such as **ACI 318-11Code**, **Eurocode 2-2004**, and **BS8110-1997** are shown in **Fig 19**.

In the **ACI 318M-11 Code,** the punching shear strength should be taken not greater than any of the following three equations:

$$P_u = 0.17 \left(1 + \frac{2}{\beta}\right) \sqrt{f_c'} \; u_o \; d \tag{1}$$

$$P_u = 0.083 \left(\frac{\alpha_s \, d}{u_o} + 2\right) \sqrt{f_c'} \; u_o \; d \tag{2}$$

$$P_u = 0.332 \sqrt{f_c'} \; u_o \; d \tag{3}$$

where, $u_o = 4(c + d)$, as shown in **Fig.19**; $\alpha_s = 40$ for symmetric punching; β = the ratio of the long side to the short side of the concentrated load or reaction area,

The equation presented in **BS8110-97**, is as follows:

$$P_u = 0.79 (100 \, \rho)^{\frac{1}{3}} \left(\frac{400}{d}\right)^{\frac{1}{4}} \left(\frac{f_{c'}}{25}\right)^{\frac{1}{3}} u_o \; d \tag{4}$$

where; $u_o = 4(c + 3\,d)$ as shown in **Fig.19**; $\left(\frac{400}{d}\right) \geq 1.0$; $25 \leq f_c' \leq 40$; $\rho \leq 3\%$

The **Eurocode 2-2004,** recommends the following expression to estimate punching shear strength of concrete slabs:

$$P_u = 0.18 \, k \, (100 \, \rho \, f_c')^{\frac{1}{3}} u_o \; d \tag{5}$$

where: $u_o = 4(c + \pi\,d)$ as shown in **Fig.19**; $k = 1 + \sqrt{\frac{200}{d}} \leq 2.0$; $f_c' \leq 50$ MPa; $\rho \leq 2\%$

In the case of ferrocement slab **Mansur and Ong, 1987**, suggested that the effective depth of slab (d) is replaced by thickness of slab (h) for the simplicity.

The above code provisions are used to calculate the ultimate punching load of normal and self compacted ferrocement slabs and the test and calculated values are summarized in **Table 5.** From this table, it can be observed that the experimental values are smaller than these calculated by ACI, Euro and BS codes. The ratio of experimental result to that calculated by **ACI**, **BS8110**, and **Eurocode 2** codes range from (0.28-0.98), (0.27-0.57) and (0.45-0.79), respectively.

Based on the test results and the above discussion, it can be concluded that these codes are unsafe and this is leaded to define specific procedure of punching shear of self compacted ferrocement slabs. For this purpose, the proposed model for punching load is given as:

$$P_u = V_u \ u_o \ h \qquad (6)$$

An empirical relation was proposed by **Mansur et al., 2001**, is used to predict the punching shear strength of ferrocement slabs (V_u). The following exponential form of equation has been selected.

$$V_u = 0.39 (f_c' V_f \frac{h}{l})^{0.5} \qquad (7)$$

The critical punching shear perimeter (u_o) of ferrocement slabs as defined by ACI code is considered as.

$$u_o = 4(c + h) \qquad (8)$$

Substituting Eqs. (7) and (8) in Eq. (6), gives a model for predicting shear load as:

$$P_u = 1.56 \ (f_c' V_f \frac{h}{l})^{0.5} \ (c + h) \ h \qquad (9)$$

A comparison of the ultimate punching shear loads predicted by Eq. (9) with experimental values is given in **Fig. 20** and **Table 5**. From **Table 5** it can be noted that the ratio of test to predicted ultimate loads ($P_u)_{test}/(P_u)_{pred.}$ ranges from 0.84 to 1.34, with an average 1.12 and a standard deviation of 0.16. Thus the proposed equation is able to predict the ultimate punching shear load of self-compacted ferrocement slabs.

5. CONCLUSION
In this paper the experimental test is made on ferrocement slabs with normal and self-compacted mortar, subjected to patch loads. Based on the results obtained from the experiments, the following conclusions may be drawn:
The load-displacement relationships for self-compacted ferrocement slabs and corresponding normal ferrocement are approximately identical at all loading stages.
The specimen with high volume fraction specimen has highest ultimate shear load and stiffness but less ductility.
Failure mode of self-compacted ferrocement slabs mainly depends on volume fraction of reinforcement and combined flexural-punching failure mode may be changed into pure punching shear with increasing the reinforcement ratio.
The ultimate shear capacity of self compacted slabs is increased by (24% and 29%) respectively, when loading plate is changed from 40 to 80 mm, respectively.
The increase of slab thickness leads to decrease in deflection values at each stage of loading and increasing in stiffness of self-compacted ferrocement slab.
 The code provisions for punching shear of structural concrete are not suitable for predicting the punching shear strength of self-compacted ferrocement slabs.

REFERENCES

➤ ACI Committee 549, 1999, *Guide for the Design, Construction, and Repair of Ferrocement*, ACI Structural Journal 85 (3), pp. 325-351.

➤ ACI Committee 318, 2011, *Building Code Requirements for Structural Concrete (ACI 318M-11) and Commentary*, American Concrete Institute, Farmington Hills, MI 48331, USA.

➤ Al-Kubaisy, M., and Jumaat, M., 1999, *Punching Shear Strength of Ferrocement Slabs*, Journal of Ferrocement, 29(2): 99-114.

➤ ASTM C 305, 1999, *Standard Practice for Mechanical Mixing of Hydraulic Cement Pastes and Mortars of Plastic Consistency*, Vol. 4, pp. 1-3.

➤ British Standards Institution (B.S.8110), 1997, *Code of Practice for Design and Construction*, British Standards Institution, Part 1, London.

➤ Dongyen, A., Sayamipuk, S., Piyarakskul, S. and Nimityongskul, P., 2006, *Strengthening of Reinforced Concrete Beam and Slab System using Ferrocement Jacketing*, Proceedings of the Eighth International Symposium and Workshop on Ferrocement and Thin Reinforced Cement Composites, 6-8 February, Bangkok, Thailand.

➤ EFNARC, 2002, *Specification and Guidelines for Self Compacting Concrete*, February, pp. 1-32, www.efnarc.org.

➤ Eurocode 2, 2004, *Design of Concrete Structures-Part 1-1: General Rules and Rules for Buildings*, CEN, EN 1992-1-1, Brussels, Belgium.

➤ Fahmy, E. H., Shaheen, Y.B. I., and Korany, Y.S., 1999, *Repairing Reinforced Concrete Columns Using Ferrocement Laminates*, Journal of Ferrocement, 29, No.2, pp. 115-124.

➤ Fahmy, E. H., and Shaheen, Y.B. I, 1994, *Laminated Ferrocement for Strengthening and Repairing of Reinforced Concrete Beams,* Proceedings of the Annual Conference of the Canadian Society for Civil Engineering, 475-483.

➤ Ibrahim H. M., 2011, *Experimental Investigation of Ultimate Capacity of Wired Mesh-reinforced Cementitious Slabs*, Construction and Building Materials, 25, pp. 251-259.

➤ Jeyasehar, C.A., and Vidivelli, B., 2006, *Behavior of RC Beams Rehabilitated with Ferrocement Laminates*, Proceedings of the Eighth International Symposium and Workshop on Ferrocement and Thin Reinforced Cement Composites, 6-8 February, Bangkok, Thailand.

➤ Kazim, T., 2012, *Viscosity and Hardened Properties of Self-Compacting Mortars with Binary and Ternary Cementitious Blends of Fly Ash and Silica Fume*, Construction and Building Materials, 37, pp. 326–334.

➢ Lub and Van, W., 1989, *Test on Strengthening of RC Beam by Using Shotcrete Ferrocement* , Journal of Ferrocement, Vol. 19, No. 4, October, pp. 363-370.

➢ Mansur, M. A., and, Ong, K. C. G., 1987, *Shear Strength of Ferrocement Beams*. ACI Structural Journal, 84(1), 10–17.

➢ Mansur, M., Ahmad, I., and Paramasivam, P., 2000 *Punching Shear Behavior of Restrained Ferrocement Slabs*, ACI Structural Journal; 97(5), pp. 765-773.

➢ Mansur, M., Ahmad, I., and Paramasivam P., 2001, *Punching Shear Strength of Simply Supported Ferrocement Slabs*, Journal of Materials in Civil Engineering; 13(6), pp. 418-426.

➢ Paramasivam, P., and Tan, K., 1993, *Punching Shear Strength of Ferrocement Slabs*, ACI Structural Journal, 7(3), pp. 294-301.

➢ Kumar, R. P., and Srikanth, K., 2008, *Mechanical Characteristics of Fiber Reinforced self Compacting Mortars*, Asian Journal of Civil Engineering, Building and Housing, Vol. 9, No. 6, 647-657.

➢ Razali, M., Kadir, A., and Noorzaci J., 2005, *Repair and Structural Performance of Initially Cracked Reinforced Concrete Slabs*, Construction and Building Material Journal; 19(8), pp. 595-603.

➢ Romualdi, J. P., Lim, C. T. E., and Ong, K. C. G., 1998, *Strengthening of RC Beams with Ferrocement Laminates*, Cement Concr. Comp., vol.20, pp. 53-65.

➢ Shannag, M.J., 2009, *High Strength Ferrocement Laminates for Structural Repair*, Concrete Solutions, Edited by Michael Grantham, Valentina Salomoni, and Carmelo Majorana, CRC Press, Taylor & Francis Group, London, U.K.

➢ Sika ViscoCrete 5930, 2010, *Product Data Sheet,* Turkey, Version no. 01.10.

NOMENCLATURE

c = side length of column, mm
d = effective depth, mm
f_c' = the compressive strength of the mortar, MPa
h = thickness of slab, mm
k = factor accounting for size effect, dimensionless
l = length of slab, mm
P_u = the ultimate punching shear load, kN
u_o = the perimeter of the critical section, mm
V_u = ultimate shear stress, MPa
V_f = volume fraction of reinforcement
w = side length of loaded plate, mm
α_s= a factor for slab column connections based on the location of the column (40 for interior, 30 for exterior, 20 for corner columns), dimensionless.

β = the ratio of the long side to the short side of the concentrated load or reaction area, dimensionless.
ρ = bending reinforcement ratio.

Table 1. Details of specimens.

Slab no.	Thickness (h) (mm)	Volume fraction Vf %	No. of wire mesh layers	Width of loading plate (w) (mm)	Compressive strength (f'c) (MPa)	Mortar type
0-45-S	45	0	0	40	70	Self compacting mortar
2-45-S		0.77	2			
3-45-S		1.154	3			
4-45-S		1.54	4			
6-45-S		2.31	6			
9-45-S		3.464	9			
2-30-S	30	1.154	2	40	71	
4-30-S		2.31	4			
6-30-S		3.464	6			
2-30-L	30	1.154	2	80	70	
4-30-L		2.31	4			
2-30-S-con	30	1.154	2	40	68	Normal mortar
4-30-S-con		2.31	4			

Table 2. Properties of wire mesh.

Specimens	Wire diameter (mm)	Yield strength (MPa)	Ultimate strength (MPa)	Modulus of elasticity (GPa)
S1	1.0	409	598	95.1
S2	1.0	392	586	94.3
S3	1.0	414	616	95.6
Average	1.0	405	600	95.0

Table 3. Fresh properties of self compacting mortar.

	Tested value of fresh mortar	**EFNARC Specification (2002)**
Mini Slump (mm)	259	Between (240 – 260) mm
Mini V-funnel (sec)	8.6	Less than 11 seconds

Table 4. Test results of slabs.

Slab no.	Mortar compressive strength (MPa)	Thickness (mm)	Load (kN)	Deflection (mm)
0-45-S	67	42	6.0	1.25
2-45-S	69	44	15.3	8.1
3-45-S	69	43	17.3	7.5
4-45-S	72	47	27.9	7
6-45-S	72	48	38	6.6
9-45-S	71	48	45.5	6.1
2-30-S	67	27	7.43	13.75
4-30-S	72	30	13.5	11
6-30-S	74	33	23.2	10
2-30-L	66	28	9.2	14.5
4-30-L	74	32	17.4	12
2-30-S-con	67	28	7.6	12.75
4-30-S-con	69	32	13.6	10.5

Table 5. Comparison of test results with codes of practice and proposed model.

Slab no.	Ultimate load (kN)					Ratio (1)/ (2)	Ratio (1)/(3)	Ratio (1)/(4)	Ratio (1)/ (5)
	Exp. (1)	ACI (2)	B.S 8110 (3)	EC-2 (4)	Pred. (5)				
2-45-S	15.3	40.53	43.5	29.91	13.9	0.38	0.35	0.51	1.10
3-45-S	17.3	39.13	48.5	32.84	16.3	0.44	0.36	0.53	1.06
4-45-S	27.9	42.54	57.54	39.12	23.0	0.66	0.48	0.71	1.21
6-45-S	38.0	47.31	73.1	50.23	29.4	0.80	0.52	0.76	1.29
9-45-S	45.5	46.32	79.31	57.34	35.8	0.98	0.57	0.79	1.27
2-30-S	7.43	19.55	24.6	14.7	6.4	0.38	0.30	0.51	1.16
4-30-S	13.5	23.52	36.27	22.1	11.6	0.57	0.37	0.61	1.16
6-30-S	23.2	27.35	45.07	29.7	17.3	0.85	0.51	0.78	1.34
2-30-L	9.2	32.43	34.22	20.51	10.9	0.28	0.27	0.45	0.84
4-30-L	17.4	40.70	51.55	31.7	20.7	0.43	0.34	0.55	0.84
2-30-S-con	7.6	20.57	25.88	15.63	6.9	0.37	0.29	0.49	1.10
4-30-S-con	13.6	25.26	33.32	24.66	12.8	0.54	0.41	0.55	1.06
Average						0.56	0.40	0.60	1.12
Standard deviation						0.22	0.10	0.12	0.16
Min. value						0.28	0.27	0.45	0.84
Max. value						0.98	0.57	0.79	1.34
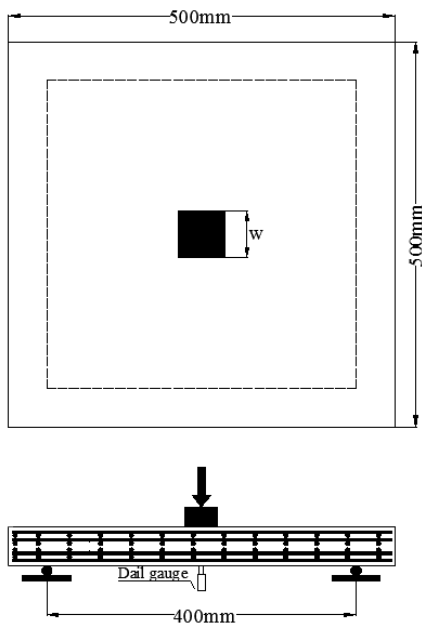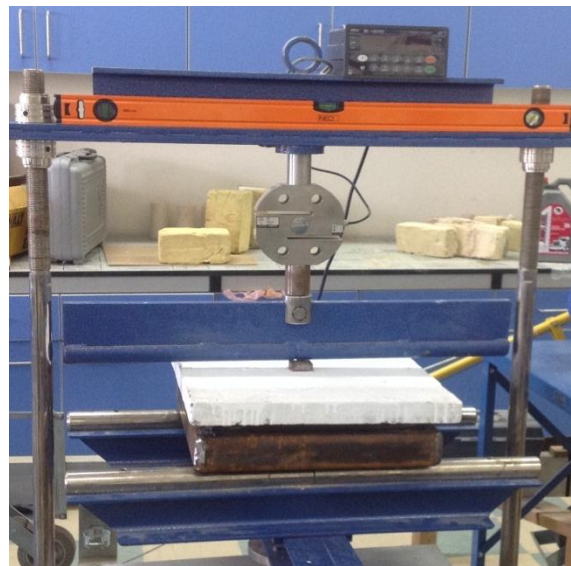
(a) Specimen detail.   (b) Test setup.

Figure 1. Specimen detail and test setup.

(a)   Mini slump cone.   (b) V-funnel apparatus.
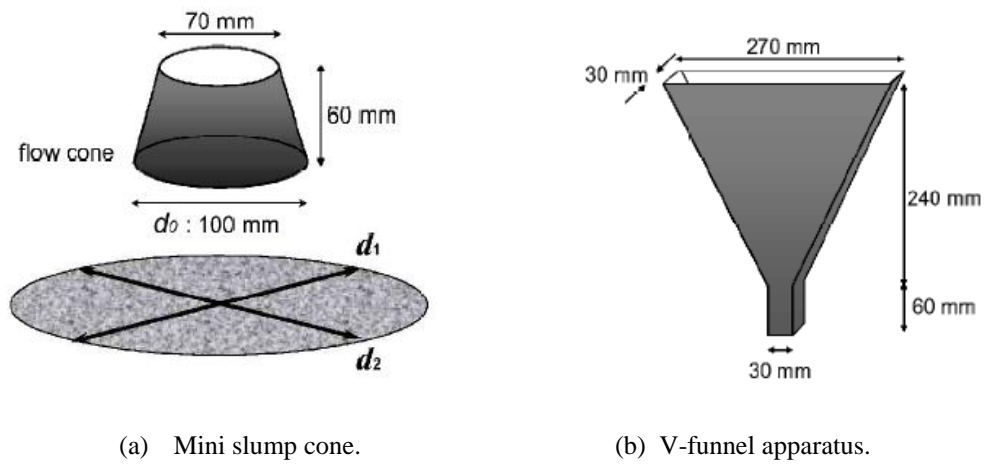
Figure 2. Mortar flow and funnel tests.

Figure 3. Fabrication and cast of self compacting specimens.
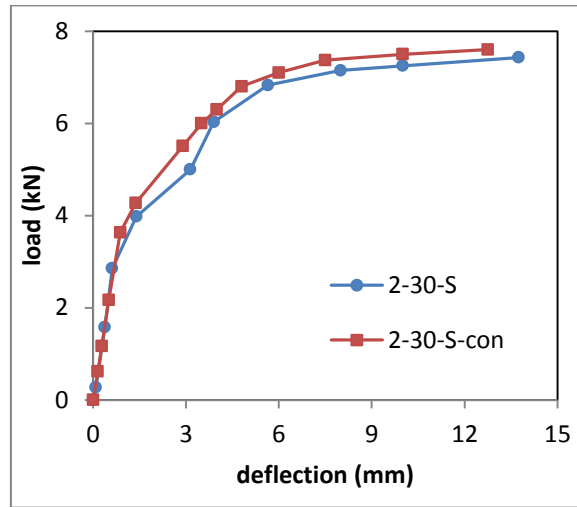
Figure 4. Comparison of load-central deflection response of self-compacted and normal slabs reinforced with Vf = 1.154%.
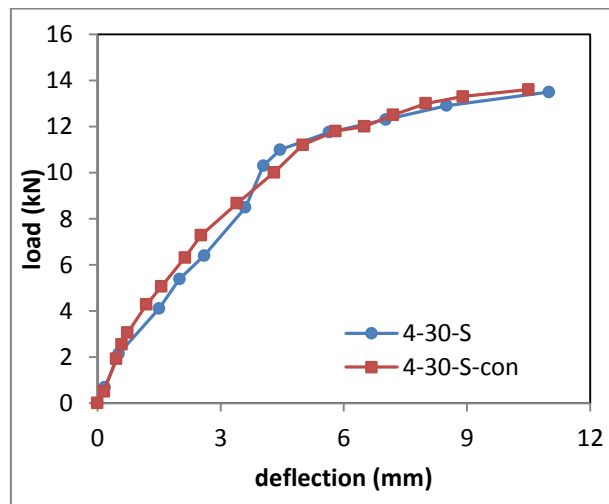
Figure 5. Comparison of load-central deflection response of self-compacted and normal slabs reinforced with Vf = 2.31%.
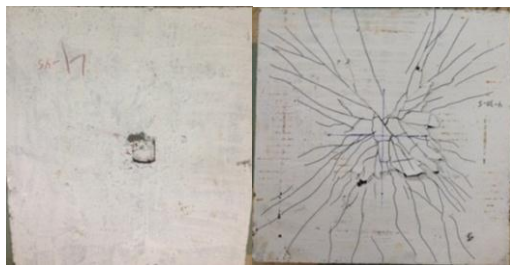
(a) 4-30-S-top face (b) 4-30-S-bottom face.   (c) 4-30-S-con-top face.   (d) 4-30-S-con- bottom face.

Figure 6. Punching failure mode of self-compacted and normal slabs.
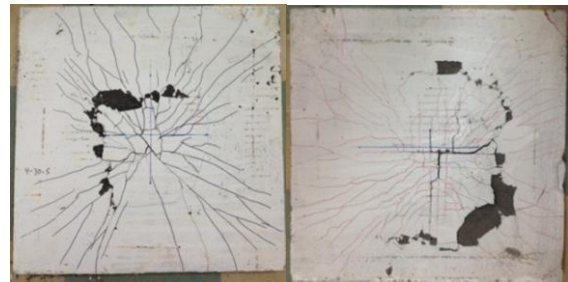
(a) 2-30-S-bottom face.   (b) 2-30-L-bottom face.

Figure 7. Failure mode of self compacted slabs with same volume fraction and different loading plate size.

(a) 4-30-S-bottom face.   (b) 6-45-S-bottom face.

Figure 8. Failure mode of self compacted slabs with same volume fraction and different thickness.

| (a) 0-45-S-bottom face. | (b) 2-45-S-bottom face. | (c) 3-45-S-bottom face. |

| (d) 4-45-S-bottom face | (e) 6-45-S-bottom face | (f) 9-45-S-bottom face |
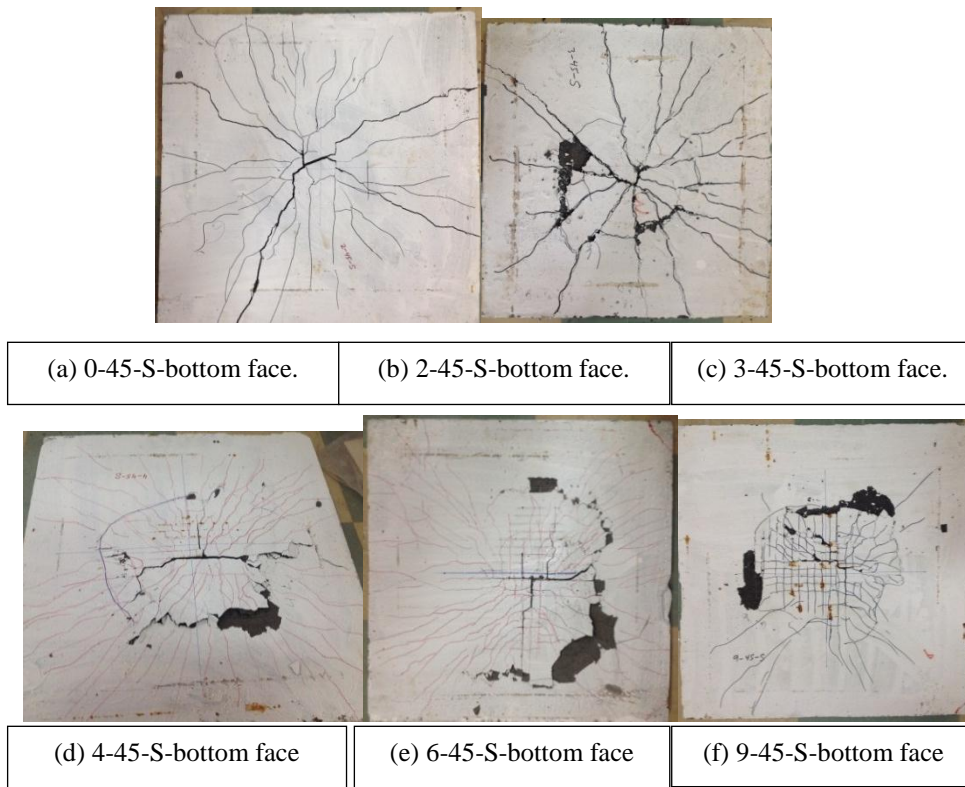
Figure 9. Failure mode of self-compacted slabs with same thickness and different volume fraction.
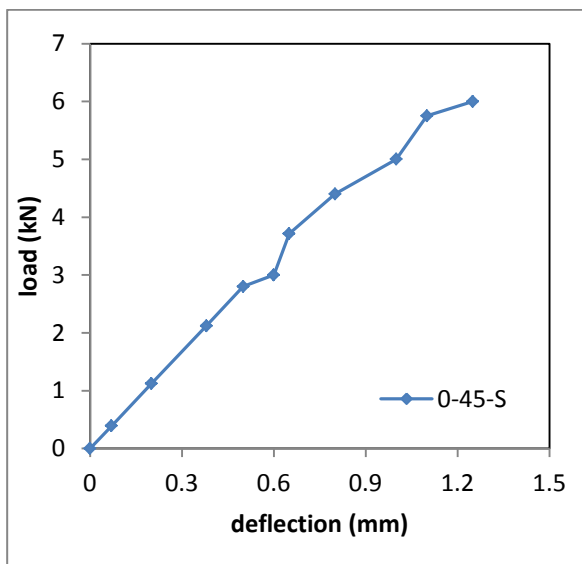
Figure 10. Load-central deflection response of plain self-compacted mortar.
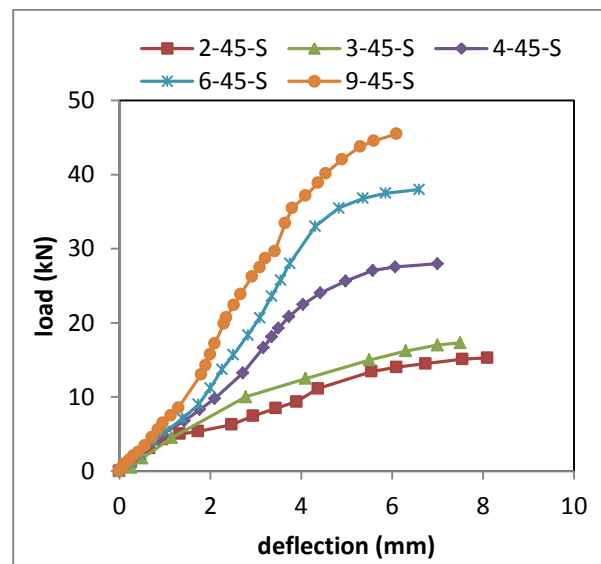
Figure 11. Comparison of load-central deflection response of self-compacted slabs reinforced with different volume fraction.
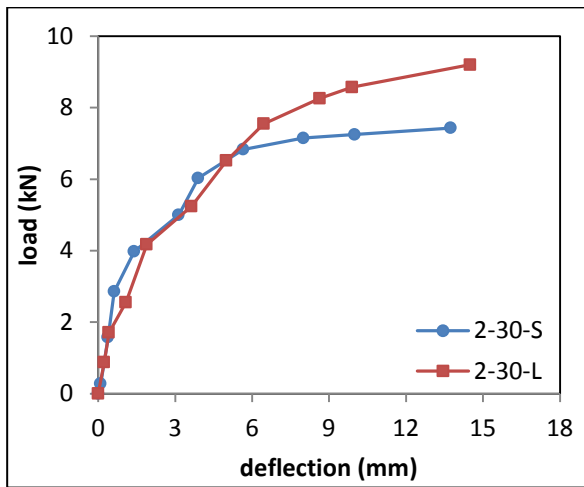
Figure 12. Comparison of load-central deflection response of self-compacted slabs reinforced with Vf = 1.154% and different loading plate size.
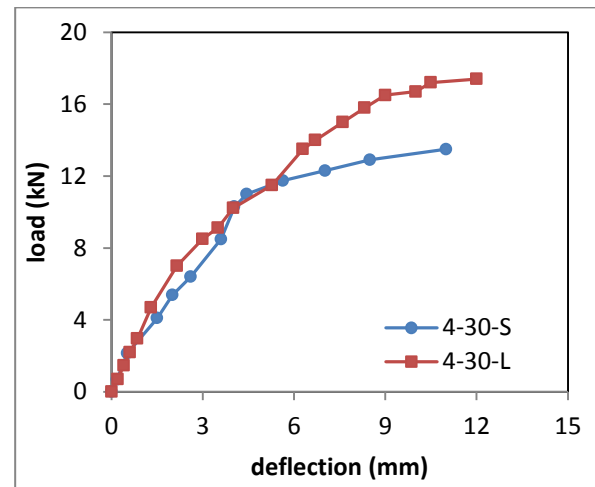
Figure 13. Comparison of load-central deflection response of self-compacted slabs reinforced with Vf = 2.31% and different loading plate size.
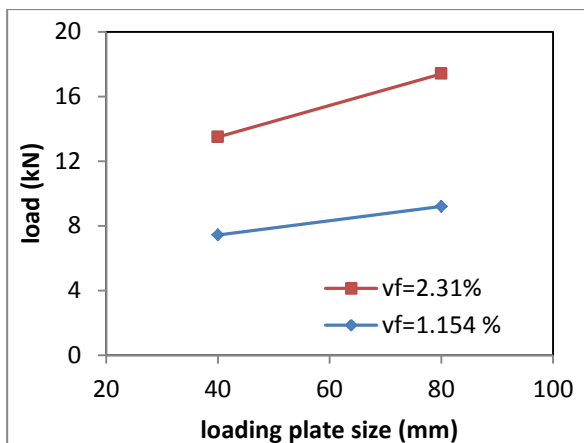
Figure 14. Effect of loading plate size on ultimate shear capacity of self-compacted slabs.
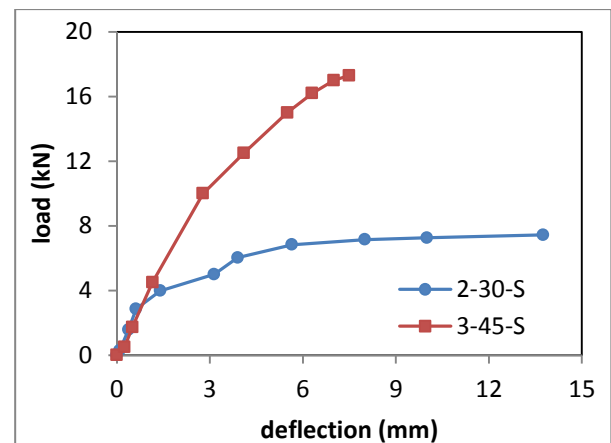
Figure 15. Comparison of load-central deflection response of self-compacted slabs reinforced with Vf = 1.154% and different slab thickness.
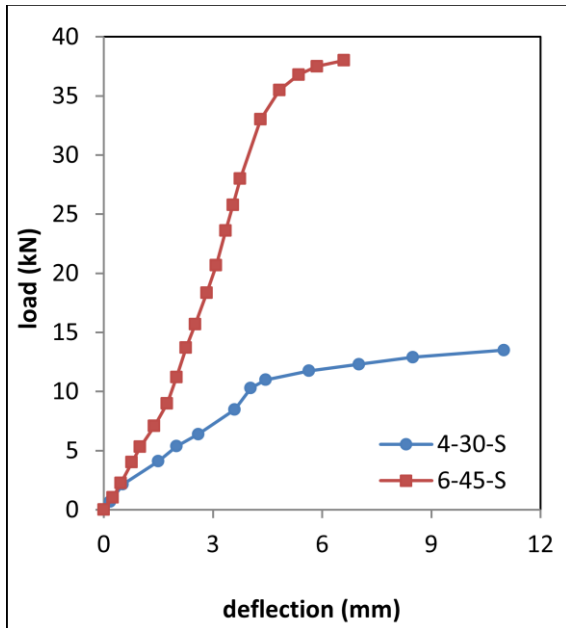
Figure 16. Comparison of load-central deflection response of self-compacted slabs reinforced with Vf = 2.31% and different slab thickness.
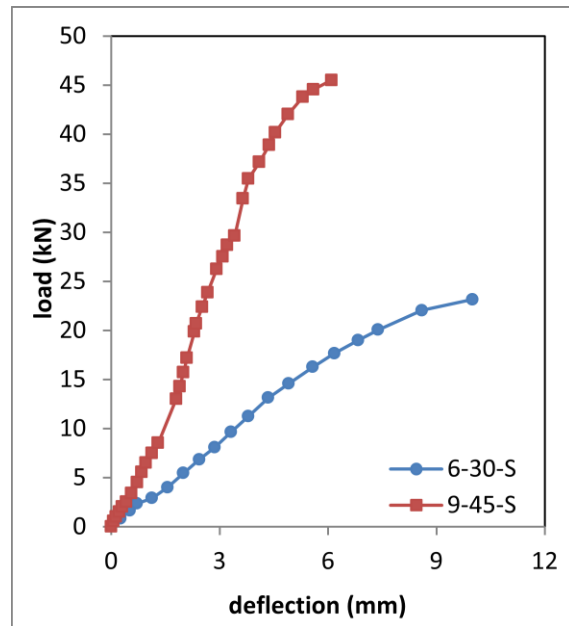
Figure 17. Comparison of load-central deflection response of self-compacted slabs reinforced with Vf = 3.464% and different slab thickness.
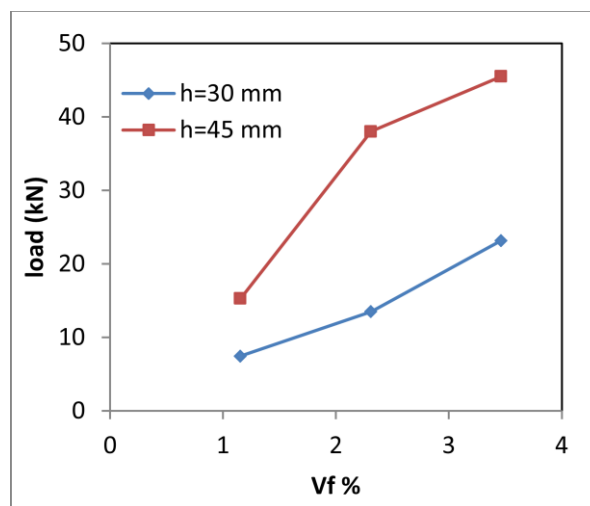
Figure 18. Effect of volume fraction on ultimate capacity of slabs.
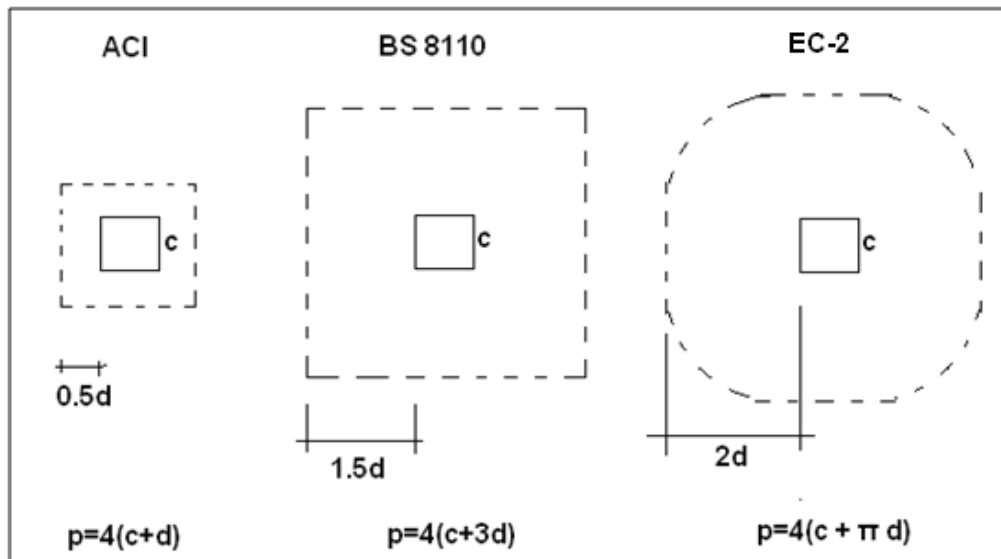
Figure 19. Critical section and perimeter of punching failure in different codes for square column.
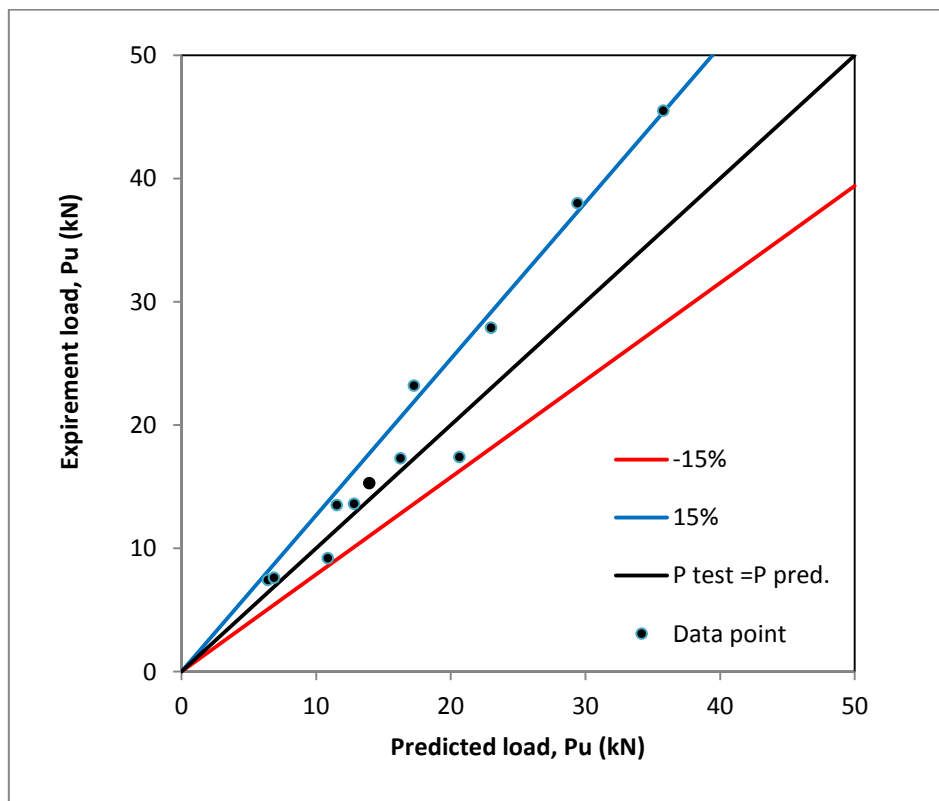
Figure 20. Comparison of experimental punching loads with prediction.